Hindawi
Mathematical Problems in Engineering
Volume 2021, Article ID 5544251, 9 pages
https://doi.org/10.1155/2021/5544251

Research Article

Deformation Investigations on the Flexspline with the Conic Curve Combined Cam Wave Generator

Shuyan Wang,[1] **Dongxiang Guo**,[2] **and Shiteng Mao**[1]

[1]*School of Mechanical Engineering, Donghua University, Shanghai 200051, China*
[2]*School of Mechanical Engineering, Jiangsu University of Science and Technology, Zhenjiang 212100, China*

Correspondence should be addressed to Shuyan Wang; shuyan@dhu.edu.cn

Received 10 February 2021; Accepted 23 April 2021; Published 5 May 2021

Academic Editor: Debiao Meng

The deformation of the flexspline and the meshing quality are largely determined by the profile of a wave generator. The wave generator with a combined profile can effectively reduce or improve the deformation stress and strain of the flexspline for improving the transmission efficiency and reducing wear or noise. In this paper, in view of the facts that conic is originally cut out of the cone and different conic curves are easy to transform, a design concept of the curve cam wave generator based on the conic curve is proposed. Firstly, the combined principle, constraint conditions, and mathematic model of the curve cam generator based on the conic curve are established. Secondly, the deformation theory of the flexspline acted by the curve cam wave generator with conic curves has been developed, and finite element analysis on stress and strain of the flexspline compared with a standard elliptic wave generator has been carried out. Finally, a cam wave generator combined with the circle and ellipse as a sample has been developed and manufactured. Circumferential strain test has been further carried out by a static strain gauge to verify the strain characteristics of the flexspline acted with the circle and ellipse combined cam wave generator. The FEM results show that, in the meshing area of the flexspline, the maximum equivalent stress of the flexspline under the action of the arc and the ellipse wave generator is about 93 MPa, which is 36.3% lower than the maximum equivalent stress of the flexspline under the action of the standard ellipse which is 143 MPa. The experimental results show that the fitting curve of the experimental results fits well with the finite element analysis curve.

1. Introduction

Compared with general gear transmission, harmonic drive has the advantages of large transmission ratio, compact structure, high contact ratio, and high efficiency, so it is widely used in aerospace, industrial robots, communication equipment, chemical machinery, and other fields such as high vacuum, corrosive, and other harmful medium space. In the harmonic drive, a wave generator forces the flexspline to produce periodic controllable elastic deformation, which can realize gear meshing between rigid wheel and flexspline to transfer power and motion [1]. Therefore, the deformation of flexspline and the meshing quality are largely determined by the profile of the wave generator.

Many investigations have focused on the profile of the wave generator and deformation performance analysis of the flexspline. Chu et al. carried out finite element analysis of harmonic gear transmission under the action of different wave generators and evaluated the meshing condition, which provides a new method for studying the interference problem of harmonic transmission [2]. Ianici and Ianici analyzed the stress distribution and displacement change of the flexspline with numerical simulations of the stress characteristics of flexspline under different loads [3]. Mahanto et al. proposed a combined wave generator, studied the stress-strain of flexspline with the combined wave generator and the traditional elliptical wave generator without rigid wheel assembly, and proved that the combined wave generator showed a better deformation distribution [4]. Compared with the traditional elliptical wave generator, the combined wave generator is mainly to meet two situations: (1) the inverse problem in the meshing theory of harmonic gear transmission. When the conjugate tooth profiles of rigid wheel and flexspline are given with traditional conjugate profile such as involute or cycloid, the profile of the wave generator needs to be solved in reverse [5]. In this way, the ready-made conjugate profile curve can be used in harmonic drive directly without increasing the difficulty of gear, which is easy to be realized in technology and can meet the production requirements. (2) The wave generator with combined profile can effectively reduce or improve the deformation stress and strain of the flexspline for improving the meshing accuracy and the transmission efficiency and reducing wear and noise.

In addition to the analysis of the profile of the wave generator and the deformation performance of the flexspline, there are also some researches on the structural design and assembling stress. Meng et al. studied the optimization method of complex engineering structure design and proposed the mean - value second-order saddle point approximation method and the first-order saddle point approximation method for offshore structure and uncertainty-based multidisciplinary design optimization problems. Engineering examples such as wellhead platform and reducer design verify the feasibility of the method [6, 7]. Yao et al. studied the influence of tooth on the bending stiffness coefficient and stress concentration factor of the tooth rim, and, through the construction of a two-dimensional rack model and performing finite element analysis, the following conclusions were drawn: root thickness and dedendum arc radius relative to the tooth rim's radial thickness are the main reflection of the article's research object. The dedendum arc radius is the main factor for the stress concentration. Finally, the correctness of the conclusion is verified by three-dimensional modeling and characteristic equations [8].

Based on the fact that the profile of the cam wave generator is very important to the deformation of flexspline, especially the influence of the cam wave generator on the number of meshing tooth pair, it is necessary to select the appropriate curve at the meshing position according to the need for better meshing performance. In this paper, in view of the diversity of conic curves and the convenience of different conic curves in combination, the profile of the wave generator designed as a combined curve with conic curves has been proposed, which can adapt to various curve saturation requirements. Based on the combination concept, theoretical analysis, numerical simulation, and finite element strength analysis on flexspline acted by the combined cam wave generator have been further developed and carried out. Then, a combined curve cam wave generator with arc and ellipse as an example has been developed and manufactured, and finally the experimental verification has been developed.

2. The Combined Profile Model of the Wave Generator with Conic Curves

The working ability of harmonic gear drive is largely determined by the deformation shape and deformation amount of the flexspline; the deformation of the flexspline is determined by the shape of the wave generator. Conic curves such as circle or ellipse are often used as hte contour curve of the wave generator, and to improve the performance of the flexspline, the combined curve cam wave generator attracted wide attention.

2.1. Conic Curves and Curve Transformation. The conic curve can be obtained by cutting the conical surface with a plane. When the inclination of the intersection plane is different, different intersection curves will be obtained, as shown in Figure 1(a). Taking the cone vertex as the origin of the coordinate system OXYZ, the equation of the conic surface is

$$x^2 + y^2 = \tan^2 \alpha \cdot z^2. \tag{1}$$

The equation of the intersection plane is

$$x \cos\beta \sin\gamma + y \cos\beta \cos\gamma + z \sin\beta = p. \tag{2}$$

Here, x, y, and z are coordinate points of the conic surface, α is the half the angle of the cone, β is the angle between the intersection plane and the Z-axis, and γ is the angle between the intersection plane and the Y-axis; p is the distance of the intersection plane from the cone convex.

From simultaneous equations (1) and (2), the equation of the intersection curve between the conical surface and the section plane can be obtained. For the convenience of the later combination curve, the equation of the intersection curve parallel to the Y-axis with $\gamma = 90^\circ$ is deduced as

$$x^2 + y^2 = \frac{\tan^2 \alpha (p - x\cos\beta)^2}{\sin^2\beta}, \tag{3}$$

and when the intersection plane is perpendicular to the axis of the cone with $\beta = 90^\circ$, the intersection curve is a circle, and the equation of the intersection curve is

$$x^2 + y^2 = \tan^2 \alpha \cdot p^2. \tag{4}$$

If there is an angle between the plane and the axis of the cone but the angle exceeds half of the cone angle with $\alpha < \beta < 90^\circ$, the intersection curve will be an ellipse.

$$\frac{\left(x + \left(\sin^2\alpha\cos\beta/\cos^2\alpha - \cos^2\beta\right)p\right)^2}{\left(\left(\sin 2\alpha \sin\beta/2\left(\cos^2\alpha - \cos^2\beta\right)\right)p\right)^2} + \frac{y^2}{\left(\left(\sin\alpha/\sqrt{\cos^2\alpha - \cos^2\beta}\right)p\right)^2} = 1. \tag{5}$$

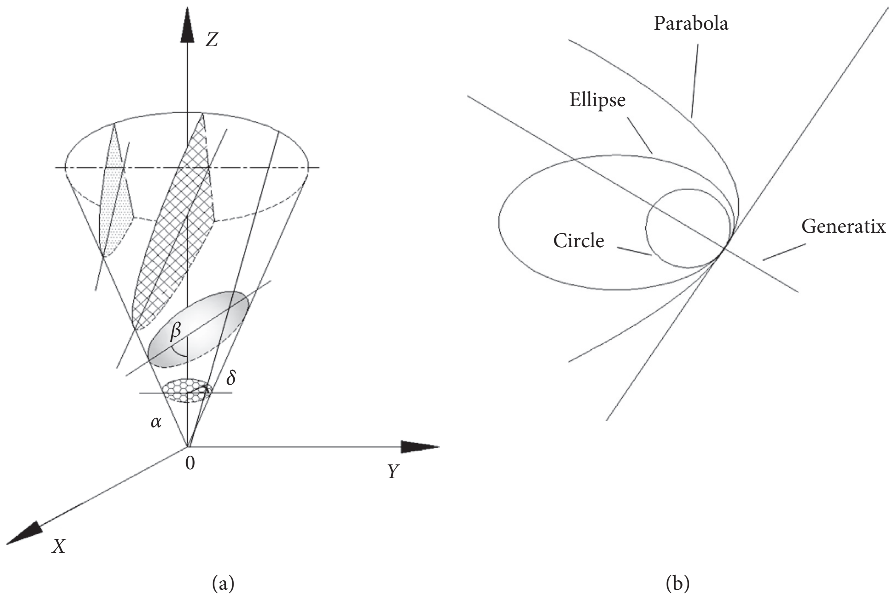

Figure 1: The generating principle of the conic curve and the transformation of conic curves along a generatrix.

If the angle between the plane and the axis of the cone equals the cone angle with $\alpha = \beta$, the intersection curve will be a parabola, and the equation of the intersection curve is

$$y^2 \cos^2 \alpha + 2xp \cos \alpha - p^2 = 0, \tag{6}$$

and if the angle between the plane and the axis of the cone is smaller than half of the cone angle ($0 \leq \beta < \alpha$), the intersection curve will be a hyperbola.

According to the generating principle of conic curve, the radius of curvature at each point of any conic curve is the same as that of the circular arc on the corresponding cross section of the cone, and the change rate is internally related to the inclination angle of the section. If a conic generatrix is taken as the baseline, moving these conic curves along the conic generatrix to a coplanar and coinciding with a point, these conic curves would tangent to a point, as shown in Figure 1(b); in a combined curve wave generator, if the curve at the meshed area is a circular arc, those conditional conjugate profiles could be chosen in harmonic drive, and the deformation problem in meshing area could be improved. Therefore, it is easier to realize the smoothness of the combined curve and the stability rate of the curvature change with the circle and other conic curves combined. In mathematics, moving and revolving these curves along the generatrix is a problem of coordinates' transformation. Here, assuming that the moving curve is the circular intersection curve, the equation of circular is deduczed as

$$(x - \Delta p \tan \alpha \cos \delta)^2 + (y - \Delta p \tan \alpha \sin \delta)^2 = \tan^2 \alpha \cdot p^2. \tag{7}$$

Here, Δp is the difference between the section of ellipse and circle from the vertex of the cone, and δ is the semi-envelop angle of arc in combined curve.

2.2. Mathematical Model of the Combined Wave Generator Profile with the Conic Curve. The mathematical model of the wave generator profile is a closed-combined-convex curve with circular arc and transition curve, and a conic curve would be chosen as the transition curve in this paper. This curve is the boundary CC of the bounded closed-convex set as shown in Figure 2, which is symmetrical along the long and short shaft of the wave generator.

In Figure 2, a sample combined curve with circles and ellipses is developed. The combined curve of the wave generator is composed of two black solid curves and two red solid curves. The dotted curve is an equivalent circle with the same circumference as the closed-combined-convex curve CC and r_m is the equivalent radius. The point D is the connecting point of a circular arc in black solid curve and an ellipse in red solid curve in the second quadrant of the coordinate system, and δ is half of the wrap angle of the circular arc curve segment. The general point Q is located at the closed-convex curve CC, and the point Q at the profile of the wave generator can be defined by a combined curve function with φ as a parameter in a polar coordinate as follows:

$$r_{CC} = r_m + \varepsilon(\varphi), \tag{8}$$

where r_{CC} is the polar radius of the point Q, $\varepsilon(\varphi)$ is the radial distance between the closed-convex curve CC and the equivalent circle, and φ denotes the polar angle of point Q.

2.3. Constraint Condition. Since the wave generator profile is the equidistant curve of the neutral layer of the flexible wheel after deformation, the profile of the wave generator in design should satisfy the following constraints:

(1) The circumference of the combined convex curve must be equal to that of the equidistant curve of the

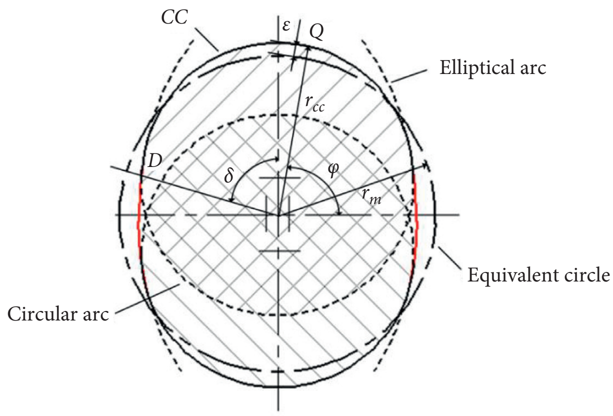

Figure 2: The combined principle with circles and ellipses.

neutral layer of the flexible wheel after deformation, and that is equal to the circumference of the equivalent circle in this paper

(2) The wave generator's long shaft must satisfy the wave height of the flexspline's deformation

(3) With the action of the wave generator, there should be no interference and no excessive clearance between the flexspline and the wheel gear on the short shaft after deformation

According to the above design constraints, the combined curve must satisfy perimeter, wave height, the boundary conditions of connection point, and an optimized short shaft. In the combined curve cam wave generator with conic curves, just the first two conditions need to be met as follows:

$$\begin{cases} L_{cc} = L_m, \\ \omega_{\max} = a - r_m, \end{cases} \tag{9}$$

where L_{cc} denotes the circumference of the closed-combined-convex curve CC, L_m is the circumference of the equivalent circle, a is the half length of wave generator's long shaft, and $\omega_{\max}$ denotes the maximum deformation on the long shaft of flexspline, also called wave height.

2.4. Case Study and Parameter Optimization of the Combined Wave Generator. According to the equation of conic curves and the constrain equation, because the circle and the ellipse are already tangent at point D, the combined curve with a circular arc and an ellipse just needs to meet the two following requirements:

$$\begin{cases} \int_{x_{B0}}^{x_D} \sqrt{1 + y'^2}\, dx + \dfrac{\delta \pi p \tan \alpha}{180} = \dfrac{\pi r_m}{2}, \\ \omega_{\max} = y_r + y_e - r_m. \end{cases} \tag{10}$$

Here, y' is the derivative of elliptic equation, y_r is the y-axis coordinate of the center point of the circle with $y_r = \Delta p \tan\alpha \sin\delta$, and y_e is the y-axis coordinate of the center point of the ellipse.

In combined curve cam wave generator, the more meshing pairs of teeth will be gained with a larger wrap angle. However, it is relatively easy to cause interference in nonmeshing area with too large wrap angle. So the size of the wrap angle would play an important role in the deformation of the flexspline. In this sample design of the combined curve cam wave generator, the half wrap angle δ could be adjusted by the length of short half shaft b_0, which would optimize the deformation of the flexspline. The relationship between the short half shaft b_0 and the half wrap angle δ of the circular arc segment is shown in Figure 3.

In our sample design, the half wrap angle δ increases with the decrease of the short half shaft b_0, but the half wrap angle is not more than 35.68° with the requirement that the circumference of the neutral layer curve of the flexspline remains unchanged. In this combined curve of wave generator with circle and ellipse, some samples of six parameters within the range of δ are shown in Table 1. In Table 1, b_0 is the half short shaft of the ellipse in the combined wave generator, b is the half short shaft of the combined wave generator, e is the offset distance of the elliptic section in the wave generator combination curve, and r is the radius of the circular arc in the combined wave generator.

3. Deformation Theory of the Flexspline

The combined wave generator with circular arc and any other conic curves force the flexspline to realize radial deformation in long shaft, which can all realize correct mesh between the flexspline and the wheel gear. Here, the forced deformation stress of the flexspline under the action of combined wave generator is deduced with the ring theory. The cross section of the flexspline is assumed to be rectangular, and the size of the cross section along the whole circumference does not change due to deformation. The circumferential strain formula of the lower gear ring of the arc and ellipse combined curve wave generator [9, 10] is as follows:

$$\begin{cases} \varepsilon_{H1} = \dfrac{h^2 w_{\max}}{6 r_m{}^3} \cdot \dfrac{1 - r_m (1 - r_m/r)/w_{\max}}{\pi/2 - \delta - \sin\delta\cos\delta} \sin\delta, \\ \varepsilon_{H2} = \dfrac{h^2 w_{\max}}{6 r_m{}^3} \cdot \dfrac{1 - r_m (1 - r_m/r)/w_{\max}}{\pi/2 - \delta - \sin\delta\cos\delta} \sin\varphi. \end{cases} \tag{11}$$

Based on the circumferential strain formulas, the circumferential strain of the flexspline acted with the combined wave generator is shown in Figure 4. Here, ε_{H1} is the circumferential strain of the circular arc section of the combined curve, ε_{H2} is the circumferential strain of the elliptical section of the combined curve, h is the wall thickness, $w_{\max}$ is the maximum radial deformation, and $\delta < \varphi < \pi/2$.

Due to the fact that there is an arc on the long half shaft of wave generator, the deformation of the flexspline in the meshing area would remain unchanged at a certain value. Compared with the standard ellipse, as long as the arc radius is larger than the curvature radius of the standard ellipse on

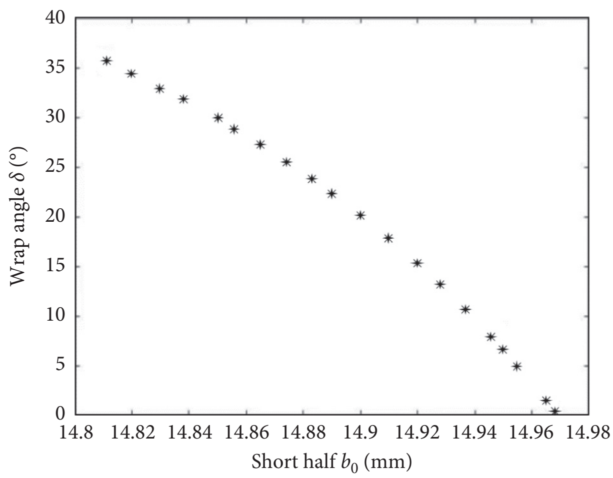

Figure 3: The relationship between the half wrap angle δ and the short half shaft b_0.

Table 1: Samples' parameters of the combined wave generator.

b_0 (mm)	a (mm)	b (mm)	e (mm)	r (mm)	δ (°)
14.968	15.32999	14.965	0.003	15.15	0.35
14.955	15.327	14.897	0.058	15.15	4.99
14.928	15.304	14.699	0.229	15.15	13.17
14.90	15.243	14.395	0.505	15.15	20.12
14.874	15.141	14.001	0.873	15.15	25.53
14.838	14.909	13.254	1.584	15.15	31.76
14.811	14.654	12.536	2.275	15.15	35.68

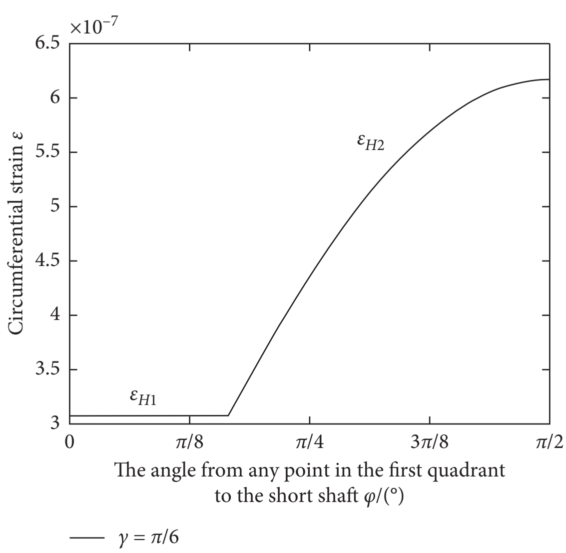

Figure 4: The circumferential strain of the flexspline acted with the combined wave generator.

the long half shaft, the deformation stress on the long half shaft of the flexspline will be reduced; that is to say, the deformation stress in the meshing area will be reduced.

4. Finite Element Analysis and Discussion of the Case Study

Numerical model of the flexspline equipped with wave generator has been developed, and the wave generator has been developed in three types of a standard ellipse profile, two eccentric wheels, and a combined curve. Then the stress and strain would be further calculated and analyzed.

4.1. FEA Simulation of the Case Study. In order to shorten the time of finite element calculation and keep the effectiveness of calculation, two simplifications are made here as follows:

(1) The tooth wall thickness of flexspline is simplified and equivalent. After simplification, the thickness of equivalent ring gear is $\delta_a = \sqrt[3]{1.67}\ \delta_b$ [11].

(2) The flexible bearing and the wave generator are regarded as a rigid body, and a rigid cylinder with equidistant curved surface of the wave generator is used to replace [12, 13].

Combined with the characteristics of the flexspline, the constraints and loads here are as follows:

(1) A fixed constraint is applied to the bottom surface of the cladding plate, and the shaft support constraint is applied to the inner hole of the flexspline

(2) The rigid outer surface of the wave generator is defined as the target surface

The three-dimensional modeling of flexspline and wave generator is developed in SolidWorks software and then imported into ANSYS for further finite analysis. The material parameters of the flexspline and wave generator are shown in Table 2. The friction coefficient between the flexspline and the wave generator is set as 0.1, and the stiffness coefficient is set as 0.1. Hexahedron cells are used to partition the calculation region of wave generator, and tetrahedron cells are used to the flexspline.

To verify the theory developed here, FEA analysis on flexspline under action of two types of cam wave generator with different parameters is developed in ANSYS environment. The FEA model of the combined cam wave generator with different parameters such as half wrap angle δ, different eccentricity, and circle radius would be analyzed to verify the theoretical study on deformation optimization.

4.2. Finite Element Assembly Analysis and Discussion. The equivalent stress of the flexspline with the standard ellipse cam and that with the combined curve cam are separately developed in Figures 5 and 6. The equivalent stress distributions of the flexspline in the tooth ring with two kinds of wave generator are shown in Figure 7. Figure 7 shows that the equivalent stress of the flexspline changes periodically. Compared with the tooth meshing area in Figures 5 and 6, it can be seen that, compared with the standard elliptical wave generator, the combined curve wave generator reduces the stress of the flexspline in the gear meshing area, which would improve the meshing accuracy, reduce wear and noise, and

Table 2: Material properties of the flexspline.

Property	Wave generator	Flexspline
Density (kg/m^3)	7850	7830
Elastic modulus (Pa)	$2.12E+11$	$2.09E+11$
Poisson's ratio	0.28	0.295
Tensile strength (MPa)	1080	980
Yield strength (MPa)	930	835

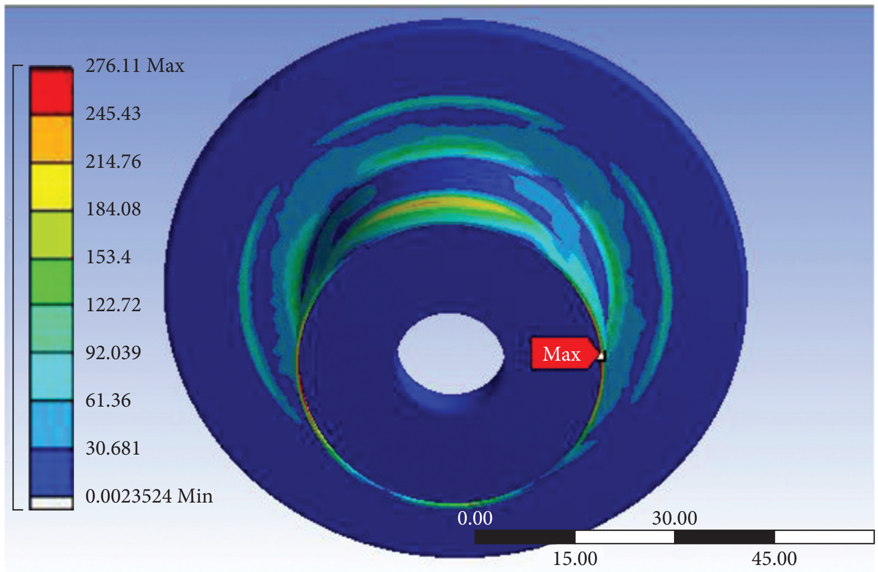

Figure 5: Equivalent stress of the flexspline with the standard ellipse cam.

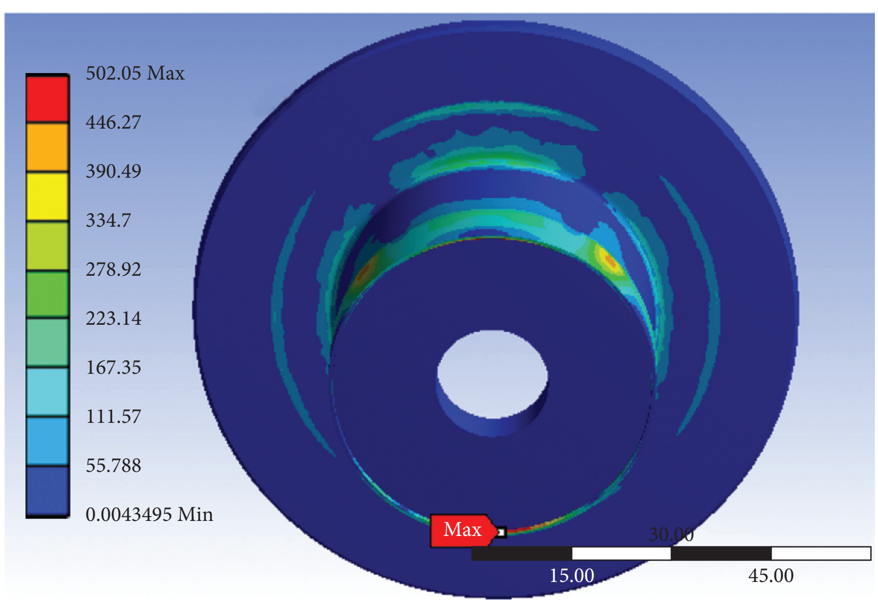

Figure 6: Equivalent stress of the flexspline with the combined curve cam.

improve the transmission efficiency. Eventually, it has reference significance for improving the service life of the flexspline in harmonic drive.

The influence of the circular arc radius of the combined curve cam on the stress of the flexspline in the meshing area is shown in Figure 8. For the flexspline with same structure size, the smaller the circular arc radius of the combined cam is, the larger the eccentricity is. If the eccentricity is too large, it is not very friendly to some tooth profiles, such as cycloid profile. It can be seen from the figure that the smaller the

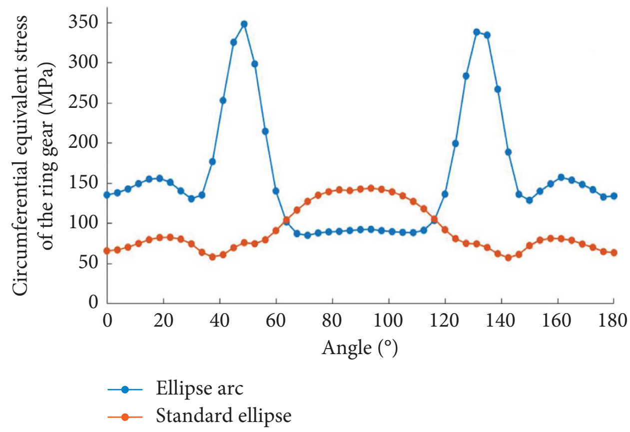

FIGURE 7: Equivalent stress distribution of the flexspline with the combined curve.

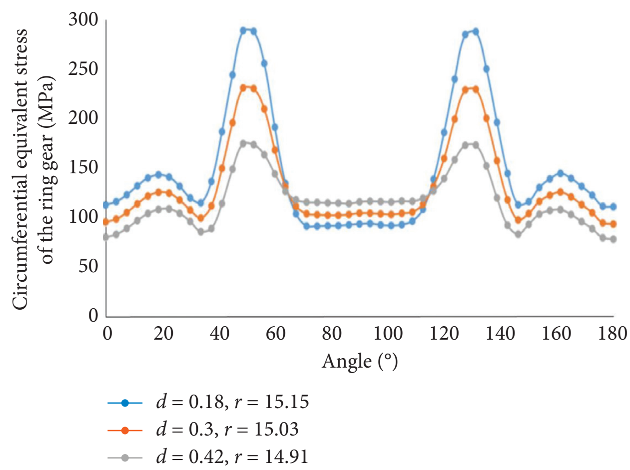

FIGURE 8: Equivalent stress of the flexspline with a standard ellipse or with different arc radii.

circular arc radius is, the larger the amplitude of equivalent stress in the ring of flexspline is, but the stress value in the meshing area will be increased. Therefore, the circular arc radius of the combined curve cam is also a main parameter to be optimized.

The wrap angle of the combined cam in the meshing area has an effect on the stress of the flexspline. The comprehensive stress would be reduced to gain beneficial effect by setting the wrap angle in a reasonable range. In this paper, the stress analysis of the combined wave generator with the wrap angle in three different values is carried out, as shown in Figure 9. It can be seen from the figure that the amplitude of the equivalent stress of the flexspline ring will be significantly reduced with the decrease of the wrap angle. This is mainly because the larger the wrap angle is, the more teeth are engaged in meshing, but the curvature change of the transition curve is more intense. This is also one of the main reasons why the stress in the nonmeshing area of the combined curve is larger than that of the standard ellipse. Therefore, choosing a reasonable arc wrap angle is an important way to balance the number of meshing teeth and the stress of flexspline.

5. Experimental Study

In order to verify the strain characteristics of the combined curve cam wave generator with circles and ellipse, circumferential strain test has been carried out by a static strain gauge. The experiment platform is composed of motor, coupling, a combined curve cam wave generator, the flexspline, and a static strain gauge, as shown in Figure 10. Because the inner ring of the flexspline is in close contact with the combined curve cam wave generator, considering the pasting requirements of the static strain gauge, the outer ring of the flexspline near the tooth is selected as the strain testing area. For measuring the circumferential strain of the flexspline, five strain gauges are designed to be uniformly pasted within 90° from the long axis to the short axis, as shown in Figure 11. The test results of test points are fitted by curve and compared with the results of finite element analysis, as shown in Figure 12. From Figure 12, it can be seen that the experiment results of the flexspline's circumferential strain acted by the combined curve cam wave generator are in good agreement with the finite element analysis results; that is to say, both the finite element analysis

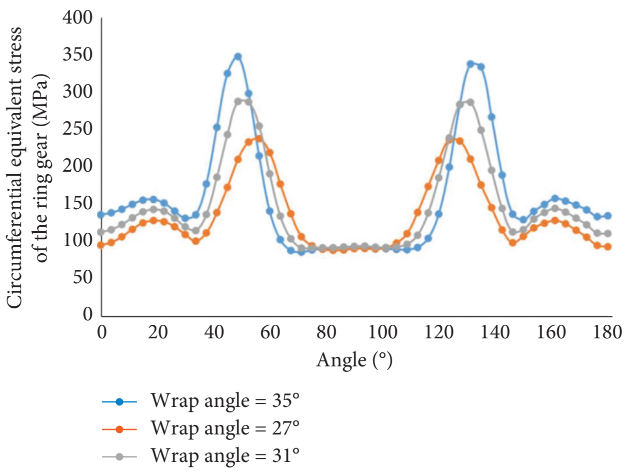

Figure 9: Equivalent stress of the flexspline with different wrap angles.

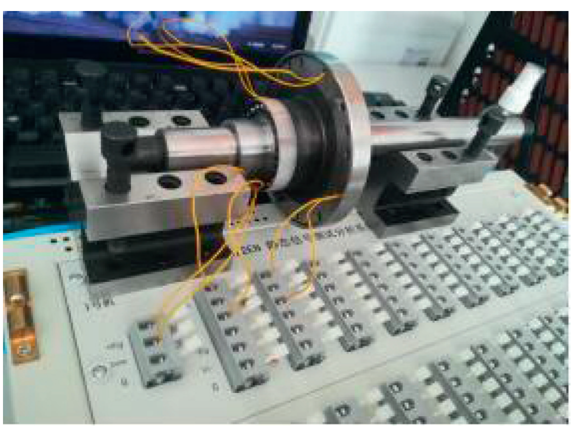

Figure 10: Partial diagram of the strain experiment system.

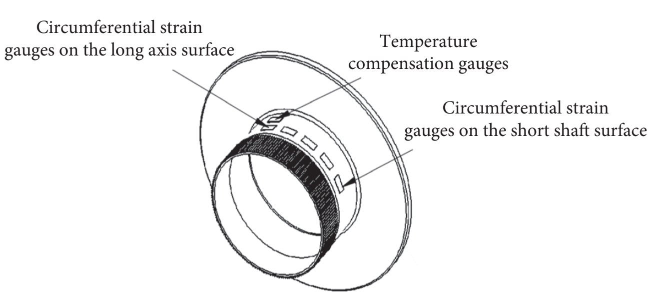

Figure 11: Location of strain gauges fixed on the flexspline gear cup surface.

and the experimental analysis show that the combined curve cam wave generator works well. Although the maximum deformation and stress of the flexspline are larger than those under the action of the standard elliptic wave generator, the performance of the combined curve cam wave generator is better than that of the standard elliptic cam in the meshing area, which is a positive significance for effectively controlling the deformation stress of the flexspline in mesh and eventually improving the service life of the flexspline.

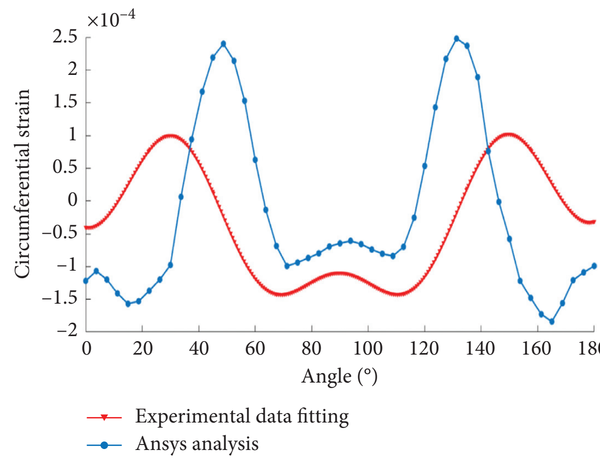

Figure 12: Comparison of finite element analysis and experimental results.

6. Conclusion

In this study, a mathematic model of combination cam wave generator based on the conic curve for investigating the stress distribution of the flexspline is proposed. This model accounts for conic curves combination and makes use of an example for stress estimation of flexspline. Moreover, the effects of arc radius, wrap angle on stress distribution, and maximum stress value are elaborately analyzed. The following conclusions can be made:

(1) Conic curves could be easily switched to achieve tangent connection satisfied with the combined principle and constraint conditions of the combined cam wave generator, and a conic-based curve combination model has been deduced. Compared with the standard ellipse cam wave generator, the stress value of the flexspline in the meshing area could be reduced, which proved that the deformation stress can be improved or reduced by using the combined cam wave generator.

(2) The equivalent stress on the gear ring of the flexspline changes periodically under the action of the combined curve wave generator, and the stress in the meshing area can be more controlled by adjusting the parameters of the arc section on the combined cam. The maximum equivalent stress increases significantly with the increase in the radius and the wrap angle.

(3) The experimental data results in the static strain experiment still have good consistency with the finite element analysis, which verifies the correctness of the theoretical analysis and finite element analysis.

Data Availability

The data used to support the findings of this study are included within the article.

Conflicts of Interest

The authors declare that they have no conflicts of interest.

References

[1] Y. Fan and B. Cao, *Technical Manual of Harmonic Gear Transmission*, National Defense Industry Press, Beijing, China, 1995.

[2] Z. J. Chu, C. Jiang, and J. Tan, "Analysis of the influence of medium wave generator on the meshing of flexspline teeth in harmonic drive," *Journal of Hangzhou University of Electronic Science and Technology*, vol. 33, no. 6, pp. 155–159, 2013.

[3] S. Ianici and D. Ianici, "Influence of the wave generator type on the stress distribution in the flexible wheel of double harmonic transmissions," *IOP Conference Series: Materials Science and Engineering*, vol. 393, no. 1, Article ID 012056, 2018.

[4] B. S. Mahanto, V. Sahoo, and R. Maiti, "Effect of cam insertion on stresses in harmonic drive in industrial robotic joints," *Procedia Computer Science*, vol. 133, pp. 432–439, 2018.

[5] X. Li, C. Song, Y. Yang, C. Zhu, and D. Liao, "Optimal design of wave generator profile for harmonic gear drive using support function," *Mechanism and Machine Theory*, vol. 152, Article ID 103941, 2020.

[6] D. Meng, Z. Hu and P. Wu, S.-P. Zhu, J. A. F. O. Correia, and A. M. P. De Jesus, Reliability-based optimization for offshore structures using saddlepoint approximation," *Proceedings of the Institution of Civil Engineers-Maritime Engineering*, vol. 173, no. 2, pp. 33–42, 2020.

[7] D. Meng, T. Xie and P. Wu, S.-P. Zhu, Z. Hu, and Y. Li, Uncertainty-based design and optimization using first order saddle point Approximation method for multidisciplinary engineering systems," *ASCE-ASME Journal of Risk and Uncertainty in Engineering Systems, Part A: Civil Engineering*, vol. 6, no. 3, 2020.

[8] Y. Yao, X. Chen, and J. Xing, "Tooth effects on assembling bending stress of flexible tooth rim in harmonic drive," *Mechanism and Machine Theory*, vol. 150, 2020.

[9] J. Fu, H. Dong, and Y. Shen, "Finite element analysis of flexspline stress in harmonic gear drive," *China Mechanical Engineering*, vol. 18, pp. 2210–2214, 2007.

[10] X. Chen, Y. S. Liu, J. Z. Xing et al., "Neutral line stretch of flexspline in harmonic driver," *Journal of Mechanical Engineering*, vol. 50, no. 21, pp. 189–196, 2014.

[11] H. Gao, Z. G. Li, and Z. Q. Deng, "Sensitivity analysis of cup-shaped flexible gear parameters to its stress based on ANSYS," *Journal of Mechanical Engineering*, vol. 46, no. 05, pp. 1–7, 2010.

[12] G. Chen, H. Li, and Y. Liu, "Double-arc harmonic gear profile design and meshing analysis for multi-section conjugation," *Advances in Mechanical Engineering*, vol. 11, no. 5, Article ID 168781401985065, 2019.

[13] J.-G. Zheng, N. Shiwei, Y.-J. Zhanghe, and L. X. Liang, "The design for the basic rack tooth profile of the harmonic gear drive with double-circular-arc," in *Proceedings of 2016 6th International Conference on Machinery, Materials, Environment, Biotechnology and Computer (MMEBC 2016)*, pp. 1738–1744, Computer Science and Electronic Technology International Society, Tianjin, China, June 2016.